

Laser-Induced Periodic Surface Structures in Polymers with Tailored Laser Fields

Rebeca de Nalda,* Maria Eugenia Corrales, Pedro Recio, Ignacio M. Casasús, Luis Bañares, Tiberio A. Ezquerro, and Esther Rebollar

In this work, laser-induced periodic surface structures (LIPSS) are generated on the surface of thin films of poly(trimethylene terephthalate) (PTT) fabricated by spin coating on silicon. Previous studies have shown the appearance of LIPSS in this type of materials with femtosecond laser pulses in the near-infrared region of the spectrum, despite the extremely low absorption of the polymer. The present work consists of an exploration of the effect of adding complexity to the femtosecond laser fields employed for irradiation. Changes in the repetition rate of the pulse train, the pulse duration, and the pulse temporal chirp are explored, and conditions for optimum LIPSS formation are identified. The effects of these modifications on the polymer surface topography, assessed by atomic force microscopy, are described and discussed.

1. Introduction

The fact that irradiation of a material surface with intense, linearly polarized laser fields can generate periodic structures through what appears to be a self-organizing mechanism was recognized shortly after the advent of the laser.^[1] The observation of laser-induced periodic surface structures (LIPSS) with periods of the order of the wavelength of the light, which are sensitive to the incidence angle and polarization, was soon recognized as a universal phenomenon capable of inducing permanent ripples in metals, semiconductors, and insulators.^[2] Initially

perceived as an unexpected laser phenomenon through a collateral effect of laser processing, it has now gained recognition as an appealing process for nanostructuring surfaces, and it has proven to be a versatile tool that allows to address challenges in diverse fields such as fluidics, optics, electronics, and medicine.^[3,4]

Significant efforts have been dedicated to LIPSS research in the recent decades, and the field of LIPSS remains a fertile ground for research. There are important challenges and numerous open questions, some of which have been examined in recent reviews.^[5] The identification of the role of the combined morphological and chemical modifications on the resulting surface properties, the control of the regularity of the LIPSS, their long-term stability, and the scalability of the process are essential for a successful transfer of the technique to industrial applications.

In particular, in the case of polymers, it has been demonstrated that surface micro- and nanostructures allow for control of optical and mechanical properties, as well as wettability by the modification of the surface energy.^[6–8] When polymers are exposed to nanosecond or picosecond laser pulses LIPSS are formed, provided they absorb at the irradiation laser wavelength, typically in the UV and visible regions.^[9–12] In the case of fs pulses, LIPSS are also formed at wavelengths at which the polymers are optically transparent.^[13,14] Unlike metals, where LIPSS can be observed after irradiation with a single laser pulse,^[15] polymers require multiple pulses, ranging from tens to thousands of pulses, to develop LIPSS.^[11,16] Previous studies have reported that, in order to form LIPSS on polymer surfaces, the material must reach its glass transition temperature (T_g) in the case of amorphous polymers or its melting temperature (T_m) in the case of semicrystalline ones.^[16] This implies that the polymer chains must flow to facilitate surface modification.


R. de Nalda, E. Rebollar
Departamento de Química Física de Materiales
Instituto de Química Física Blas Cabrera (IQF-CSIC)
Serrano 119, 28006 Madrid, Spain
E-mail: r.nalda@csic.es

M. E. Corrales
Departamento de Química
Facultad de Ciencias, Módulo 13
Facultad de Ciencias
Universidad Autónoma de Madrid
28049 Madrid, Spain

P. Recio, I. M. Casasús, L. Bañares
Departamento de Química Física (Unidad Asociada I+D+I al CSIC)
Facultad de Ciencias Químicas
Universidad Complutense de Madrid
28040 Madrid, Spain

L. Bañares
Instituto Madrileño de Estudios Avanzados en Nanociencia (IMDEA-Nanoscience)
Cantoblanco, 28049 Madrid, Spain

T. A. Ezquerro
Departamento de Física Macromolecular
Instituto de Estructura de la Materia (IEM-CSIC)
Serrano 121, 28006 Madrid, Spain

 The ORCID identification number(s) for the author(s) of this article can be found under <https://doi.org/10.1002/pssa.202300721>.

© 2023 The Authors. physica status solidi (a) applications and materials science published by Wiley-VCH GmbH. This is an open access article under the terms of the Creative Commons Attribution-NonCommercial-NoDerivs License, which permits use and distribution in any medium, provided the original work is properly cited, the use is non-commercial and no modifications or adaptations are made.

DOI: 10.1002/pssa.202300721

Environment can influence LIPSS formation. For instance, the size of LIPSS formed on metallic films can vary when irradiated in different liquids compared to the irradiation in air.^[17] Also, the bulk temperature plays a role in LIPSS formation on the surface of polycarbonate films, as higher temperatures result in a stronger absorption of laser energy by the polymer.^[18] Additionally, the formation of LIPSS may also be influenced by the thickness of the material film or the nature of the substrate on which the material is supported.^[19–23]

Besides the material and the environmental properties, the characteristics of the applied laser irradiation play a defining role on LIPSS formation. The laser fluence and the number of pulses influence both the period and the quality of the resulting nanostructures,^[4] and the laser wavelength also determines the period, while the polarization determines the direction of the LIPSS. Additionally, it has been found that the beam wavefront curvature plays a role on the regularity of the laser-fabricated LIPSS.^[24]

Furthermore, the properties of LIPSS can be fine-tuned by manipulating the temporal features of the laser pulses. In particular, LIPSS formation is clearly influenced by the laser pulse duration. When using ns or longer pulse durations and irradiating at normal incidence, the resulting low-spatial frequency LIPSS (LSFL) typically exhibit periods very close to the irradiation wavelength. However, for ultrashort laser pulses, reported periods often range between 0.7λ and 0.9λ and can be influenced by the number of laser pulses applied.^[25] High-spatial frequency LIPSS (HSFL) with periods much shorter than λ are exclusively observed when using ultrashort laser pulses. These ultrashort pulse durations are typically below the specific electron–phonon relaxation times of solids, which hinders significant heat dissipation from the regions where energy deposition is produced during irradiation.^[4] Dzienny et al. reported that the nanoripples obtained with nanosecond irradiation are shallow and smooth in comparison with those formed with pico- and femtosecond pulses, due to the melting and surface oxidation in case of ns irradiation,^[26] while Bashir et al. investigated the formation of LIPSS on zirconium using laser pulses with durations ranging from 25 fs to 100 fs.^[27] Keeping the number of pulses and the pulse energy constant, LIPSS were better formed for the shortest pulse duration of 25 fs. To our knowledge, the behavior of LIPSS as a function of the sign of the pulse chirp has only been reported once for the case of a ceramic material by Kakehata et al.^[28]

Other features of the pulse structure have also demonstrated their influence on LIPSS. For example, different research groups have investigated the effect of temporal delays in double-fs-pulse sequences,^[29–31] the energy distribution within pulses,^[32] the relevance of the polarization direction and the wavelength in double-pulse sequences,^[33] and even the application of more than two pulses within each sequence.^[34] Additionally, the role of the repetition rate has also been examined for LIPSS formed in silicon.^[35,36] The behavior of LIPSS in polymers as a response to the features of the ultrashort laser pulse train has only been scarcely studied.

In this work, LIPSS have been generated on the surface of thin films of poly(trimethylene terephthalate) (PTT) fabricated by spin coating on silicon. Previous studies had shown the appearance of LIPSS in this type of materials with femtosecond laser pulses in the near-infrared region of the spectrum,^[13,14] despite the

extremely low absorption of the polymer. The effects of repetition rate and pulse duration have been explored, and an investigation of the role of the sign of the group velocity dispersion, or pulse chirp, has been undertaken. The effects of introducing these changes in the nature of the laser pulse train on surface topography are described and discussed, and as a result, the conditions for optimum LIPSS formation have been identified.

2. Results and Discussion

Irradiation of the PTT samples with sequences of $5\text{--}20 \times 10^4$ pulses (with pulse energies in the region of $400\text{--}600 \mu\text{J}$, corresponding to a fluence region of $20\text{--}40 \text{ mJ cm}^{-2}$) produced periodic surface structures along the direction parallel to the polarization axis of the laser beam. A typical example of such structures can be seen in the atomic force microscopy image shown in **Figure 1a** for the central part of an irradiated region. As is typical of short pulse irradiation of this type of material,^[26] the surface also presents some granularity in the direction perpendicular to the polarization direction, but no periodicity is present along this dimension.

The analysis of the images was performed by averaging the atomic force microscopy (AFM) height data across vertical lines in a box of the image typically sized $6 \mu\text{m}$ (horizontally) by $1 \mu\text{m}$ (vertically). Sinusoidal functions were used to fit the obtained curves, with period and amplitude as free parameters. The procedure was repeated several times so that errors could be estimated from statistical analysis. The study of the AFM images yields depth profiles like that shown in **Figure 1c**. From the fit of the parameters of a sine function to the experimental data, values of the period and amplitude of the topographic structures can be obtained. Measured periods are found to be slightly below the radiation wavelength, as is expected from low-spatial frequency LIPSS at normal incidence.^[13] The modulation of the depth is of the order of the sample thickness, indicating that the process involves the whole polymer thin film. **Figure 1b** shows the edge of the modified region in a similar situation. It shows that the onset of the strong depth modulation is rather sharp, taking place across a few hundred nanometers. Also, it reveals that the process involves material reorganization, since different parts of the newly generated surface lie both above and below the untreated material. As has been observed previously,^[37] self-standing films of this polymer do not show the appearance of LIPSS under short-pulse near-infrared irradiation. Therefore, the Si substrate on which the thin films are deposited plays a crucial role in the formation of the structures.

2.1. Role of the Pulse Train Repetition Rate

The study of the role of repeated illumination was undertaken by varying the repetition rate of the pulse train while keeping the total number of pulses applied to a target region constant. Thus, starting from a reference situation where each sample region was irradiated at 1 kHz over a period of 10 s, the repetition rate was reduced by factors of 2, 5, 10, 20, 50, 100, and 200, obtaining frequencies of 500, 200, 100, 50, 20, 10, and 5 Hz, respectively, and exposure times were increased by the same factors so that all regions received a total of 10,000 laser shots.

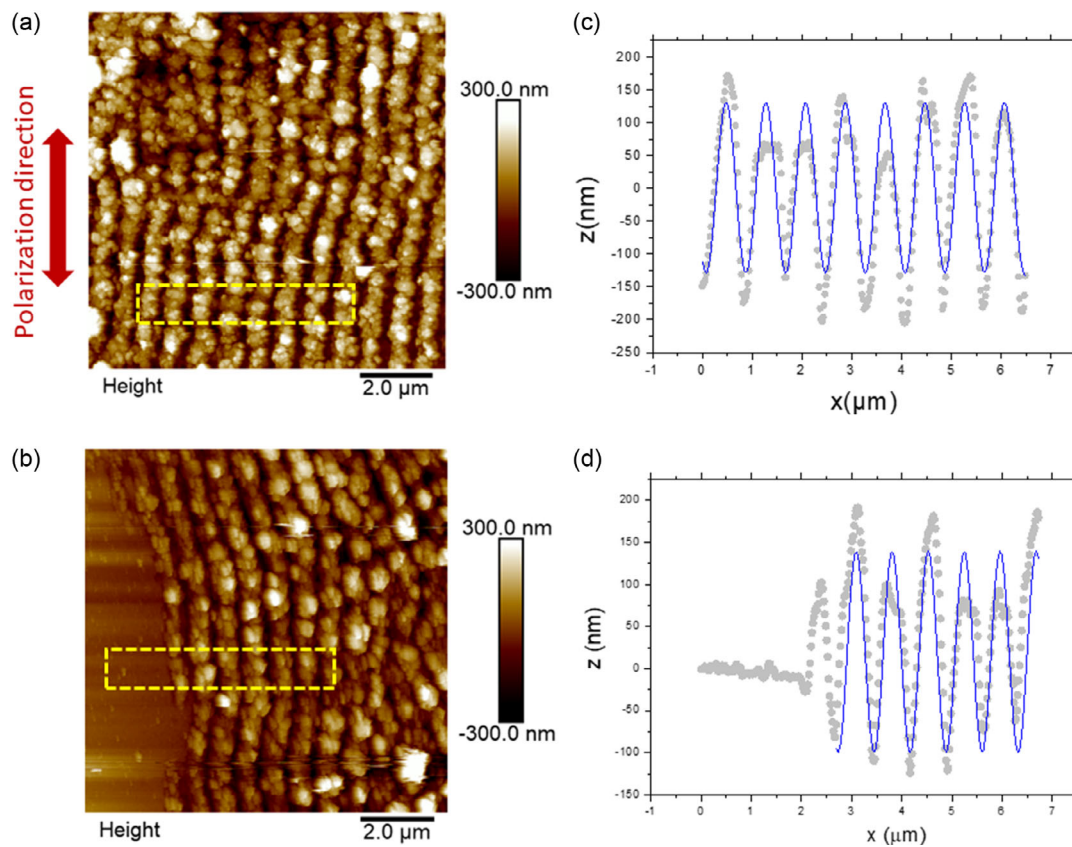


Figure 1. LIPSS formed on the surface of PTT upon fs laser irradiation. The double arrow indicates the polarization direction of the laser. a) AFM image of zone irradiated with 10,000, 600 uJ pulses at 800 nm central wavelength, 1 kHz repetition rate. b) AFM image of the edge of a zone irradiated with 20,000, 460 uJ pulses at 800 nm central wavelength, 1 kHz repetition rate. c,d) Profiles of the surfaces obtained upon integration across the direction parallel to the laser polarization in the boxes indicated with a dashed yellow line on (a) and (b), respectively. The grey dots are the values obtained from the measurement; the blue line corresponds to a fit to a sine function.

Figure 2 shows a selection of the topographies obtained with this procedure. We observed that 1 kHz and 500 Hz produced very similar surface structures. However, further decreasing the repetition rate to 200 Hz or below, corresponding to interpulse delays of 5 ms or longer, was deleterious for the generation of periodic structures. Instead, a granular structure was observed in these cases. Only a selection of the images obtained for these lower repetition rates are shown in the figure, since very similar results were measured for repetition rates between 5 Hz and 200 Hz.

These results show that the interpulse delay in the pulse train is a crucial parameter for the formation of periodic structures. They suggest that heat accumulation, which cannot happen if the interpulse delay is long -i.e., if the repetition rate is low- is essential for the formation of LIPSS. We find the transition from the formation of LIPSS to their disappearance between 500 Hz and 200 Hz, that is, between 2 ms and 5 ms interpulse delay in this case. The value of the thermal diffusivity of PTT is very low ($1.2 \times 10^{-7} \text{ m}^2 \text{ s}^{-1}$),^[9] and that of the Si substrate is moderately low too ($9.97 \times 10^{-5} \text{ m}^2 \text{ s}^{-1}$), which causes a very slow cooling process after each laser shot. The one-dimensional model applied in ref. [19] for a similar situation shows expected temperature decay times compatible with the range of 10^{-3} s found here for polymer layers of the order of 200 nm. For

PTT, interpulse delays shorter than 5 ms are thus necessary for the heat accumulation required to overcome the glass transition, allowing periodic material reorganization. It is conceivable that this parameter shows a window effect, in that higher repetition rates, at the same pulse energy and number of pulses, may cause a temperature increase so large that it may prevent the formation of organized structures, but the limitations of the experiment, where the maximum attainable repetition rate was 1 kHz, did not allow this exploration. To our knowledge, no previous work on the role of the repetition rate on LIPSS formed on polymeric materials exists. However, Mezera et al.^[18] explored a related parameter: the role of the bulk polymer temperature. Their observation showed that preheating the polymer reduced the required laser fluence for the formation of LIPSS, and this was interpreted through the idea that, in a preheated polymer, less energy deposited by the laser is required to reach the glass transition temperature. This is applicable to the situation described here where higher temperatures are only attained through higher repetition rates, i.e., shorter interpulse delays that do not allow for sufficient cooling time.

In non-polymeric materials, the laser pulse train repetition rate was extensively studied in relation to LIPSS by the group of Amoroso and co-workers for the case of silicon.^[36] A relevant

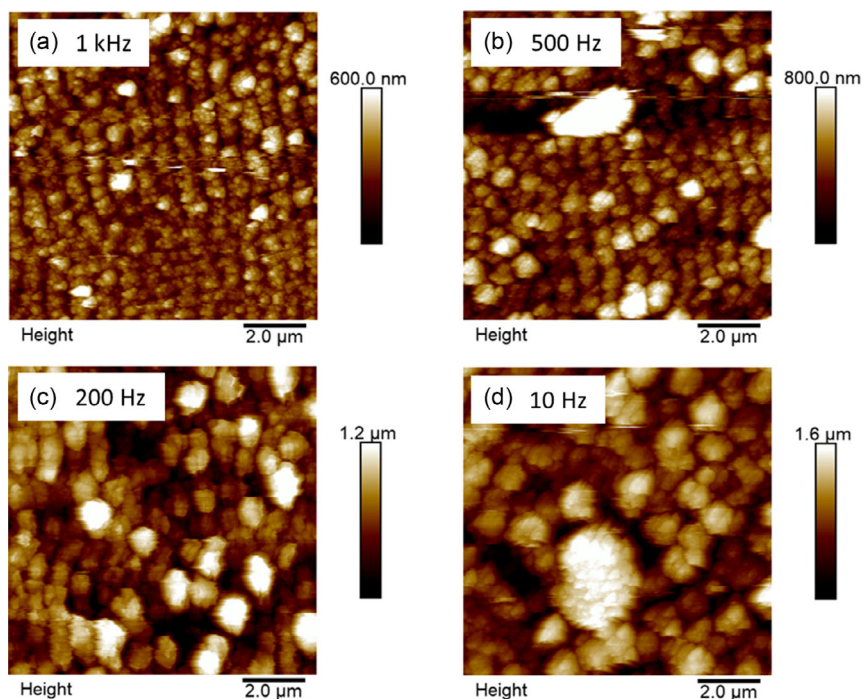


Figure 2. AFM images of PTT irradiated with 10,000 laser shots at single pulse energies of 520 μJ . The four images correspond to different repetition rates and exposure times, as follows: a) 1 kHz, 10 s exposure; b) 500 Hz, 20 s exposure; c) 200 Hz, 50 s exposure; d) 10 Hz, 1000 s exposure.

finding in those works was the deleterious role of plasma shielding when high repetition rate trains were employed in air, which set a maximum repetition rate of 10 kHz for successful LIPSS generation. In the experiment described in this work, the repetition rates have always been kept below 10 kHz, but even if higher rates had been used, we do not believe that plasma shielding would play an important role, since our processing conditions take place well below the ablation threshold, as opposed to the works by Amoruso et al.

2.2. The Role of the Pulse Duration and Chirp

The second type of experiment that was undertaken to understand the role of the details of the irradiation field on the generated surface patterns was the introduction of nonzero group velocity dispersion in the laser pulses and the observation of the resulting surface modification. Introduction of chirp was done by de-optimizing the distance between the diffraction gratings in the compressor of the laser after amplification as is explained

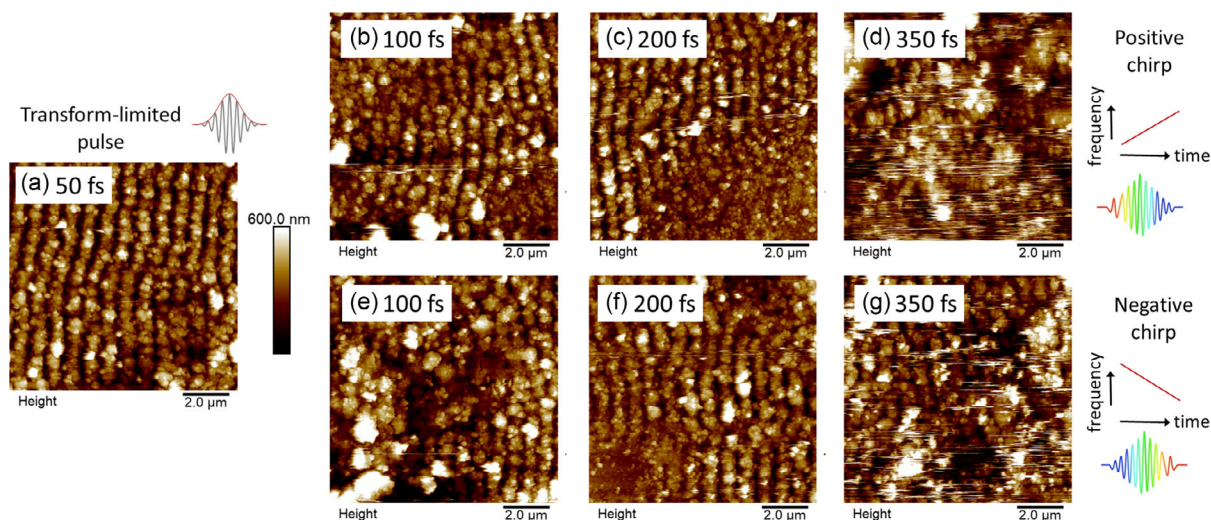


Figure 3. AFM images of irradiated PTT with trains of 10,000 NIR pulses at 1 kHz repetition rate and 600 μJ single pulse energy, for a range of pulse durations obtained by introducing either positive or negative chirp. a) Transform-limited pulses of 50 fs duration; b–d) Pulses with positive chirp, with a duration of 100, 200 and 350 fs, respectively; e–g) Pulses with negative chirp, with a duration of 100, 200 and 350 fs, respectively.

in the experimental section, producing up-chirped or down-chirped pulses depending on whether the grating distance is made longer or shorter than optimum. In this way, pulses with durations of 100, 200, and 350 fs were synthesized and diagnosed, both with up-chirp and down-chirp.

The results of applying sequences of these chirped pulses on the PTT surface are shown in **Figure 3**. In all cases, sequences of 10,000 pulses at 1 kHz repetition rate and with pulse energies of 600 μJ were applied. As can be appreciated, periodic structures were generated on the sample surface for the transform-limited pulse and for pulses that were temporally stretched up to the value of 200 fs. Beyond this pulse duration, even though roughness appears on the surface, no clear periodicity can be detected. For each given pulse duration, the structures appear similar for up-chirp compared to down-chirp. Separate experiments were conducted for different total irradiation times, with similar results. Also, the observations in further experiments conducted at lower pulse energies (520 μJ) were also compatible with those described here.

In order to quantify the observed changes, the periods and amplitudes of the structures generated for each of the pulse durations employed, both with positive and negative chirp, and for different values of the total exposure time, have been analyzed and are shown in **Figure 4**. The graph has included data for 50, 100, and 200 fs pulses, since those of 350 fs duration do not produce structures with sufficient order to be analyzed. In all cases, data for negatively chirped pulses are shown with solid symbols and data for positively chirped pulses, with open symbols. Total exposure times are indicated in the figure. It can be seen that both periods and amplitudes of the structures generated in the different conditions are compatible with the error bars. Therefore, a value of the average period and amplitude has been obtained and plotted on the figure, with an indication of the standard deviation with a shaded-grey area. The period measured from this global average has a value of 750 ± 35 nm, whereas the obtained amplitude is 195 ± 40 nm, from which we can note that the determination of the period is significantly more precise than the determination of the amplitude of the surface structure. The scatter of the data with respect to the central value is higher for the longer, 200 fs pulses, probably revealing the progressive loss of order as the pulse length is increased.

The loss of order of generated LIPSS as the pulse duration is increased in the tens-to-hundreds of femtoseconds range was reported previously by Bashir et al. in experiments in zirconium immersed in a liquid,^[27] and also on Zn in air and ethanol,^[38] with results that indicate best response of the nanostructure formation with shorter, and thus more intense pulses, in the same direction that we have found in this work for the polymeric material deposited on Si.

As mentioned previously, the Si substrate plays a crucial role in the formation of the LIPSS in the polymer, and the observation of a quasi-constant LIPSS amplitude is an indication that LIPSS are only observed when the whole thin film is involved in material reorganization. Further, in a separate set of experiments, it was observed that self-standing PTT films do not show LIPSS under similar irradiation conditions.^[37] We believe that the formation of LIPSS in thin films of PTT on silicon may be related to the coupling of the laser light with surface plasmon polaritons (SPPs) expected to appear at the interface between the dielectric polymer and the substrate. The role of SPPs in the formation

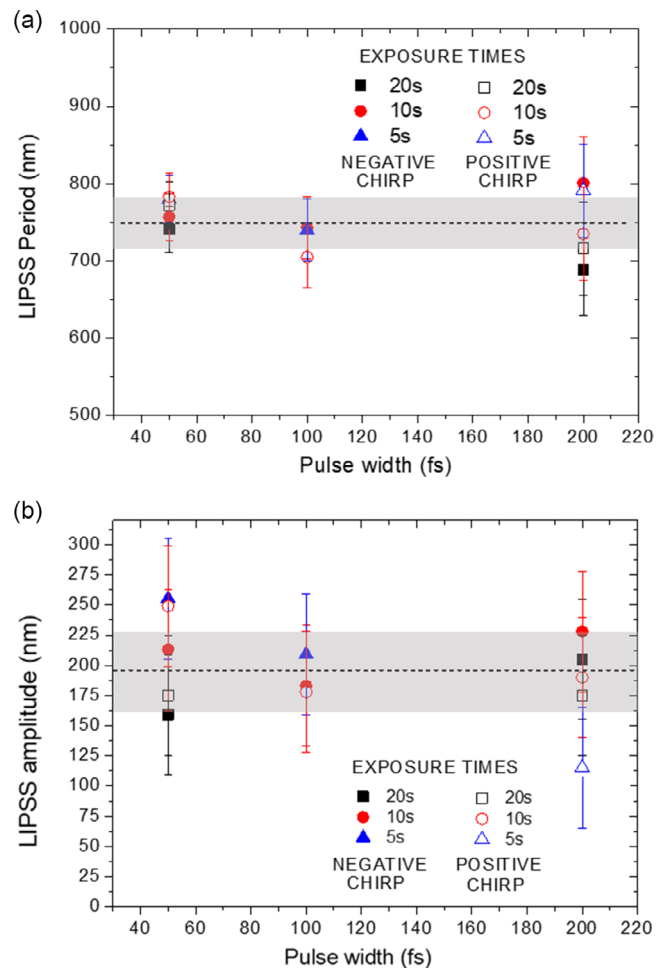


Figure 4. Periods a) and amplitudes b) of the LIPSS formed on PTT with either negatively chirped pulses (solid symbols) or positively chirped pulses (open symbols). The labels beside the symbols indicate exposure time, where 20, 10, and 5 s are indicated with squares, circles and triangles, respectively. The dotted horizontal line on each graph indicates the average of all measurements, with shadowed area showing one standard deviation.

of LIPSS in thin polymeric films was explored in^[23] for the case of gold substrates. The authors concluded that the generation of SPPs on the polymer/Au interface giving rise to a periodical field pattern on the surface of the thin film caused an inhomogeneous temperature rise on the surface of the sample and constituted the main mechanism underlying the formation of LIPSS in these systems. Although SPPs are primarily described at metal/dielectric interfaces,^[39] they may appear in a dielectric/Si interface due to metallization of the character of the Si substrate, as was discussed by Nürnbergger et al.^[40] for the case of layers of SiO_2 on Si. It is important to note, however, that if interference with the SPPs was directly imprinted on the polymeric layer, then it would be expected that the direction of the ripples would be perpendicular to the laser polarization axis, as was indeed observed in the SiO_2/Si work.^[40] Instead, the fact that the ripples observed in the PTT film are parallel to the laser polarization points to a less direct mechanism causing temperature modulation on the film due to substrate excitation.

The introduction of chirp in the individual laser pulses, with the subsequent stretch in pulse duration, despite maintaining the laser fluence constant, causes a decrease in the peak laser intensity. The observation that ordered LIPSS disappear for these longer pulses suggests that nonlinear effects play a role. One possibility is that, for longer pulses, the sample does not reach a temperature that is high enough for material reorganization. However, the high induced roughness seems to indicate otherwise, so we believe that the loss of order is rather related to the dispersion in the periods, which would prevent the emergence of a periodic structure.

Regarding the influence of the sign of the GVD, or pulse chirp, we have found scarce information in the literature,^[28] and none concerning polymers. In the article by Kakehata et al., describing laser processing of a ceramic material, the authors report a significantly varying LIPSS period with pulse duration, which is in contrast to the present work for the PTT polymer. However, their findings are not dependent on the sign of the chirp, as was observed for the case described in the present work.

3. Conclusion

LIPSS have been successfully generated on the surface of thin films of PTT fabricated by spin coating on Si through near-infrared irradiation with trains of ultrashort laser pulses. Ripples with spatial periods slightly below the laser wavelength, and depth close to the full film thickness have been fabricated in a single-pulse fluence range of 20–40 mJ cm⁻² after the application of several thousand pulses. It has been concluded that in these conditions the Si substrate plays a crucial role in the formation of the ripples. The study of the features of the structures as a function of the pulse train repetition rate has revealed that trains with a temporal spacing longer than 2 ms are not adequate for the generation of the periodic structures, which has been ascribed to the absence of heat accumulation effects necessary to allow for material reorganization. A study of the effect of pulse duration revealed that the structures present optimum contrast and regularity for the shortest 50 fs pulses used, and also for moderately stretched pulses to 100 fs pulse width. Further stretching of the pulses gave rise to less regular structures, until for pulses beyond 300 fs periodic ripples were no longer visible. No differences in the generated LIPSS could be observed for a given pulse duration for different signs of the group velocity dispersion in the pulse.

4. Experimental Section

PTT was synthesized by polycondensation as previously described.^[41] Molecular weight, determined by size exclusion chromatography (SEC), is $M_n = 31\,294\text{ g mol}^{-1}$, with a polydispersity of $M_w/M_n = 2.22$. PTT is a semicrystalline polymer, with a melting temperature $T_m = 229\text{ }^\circ\text{C}$. It can be quenched from the molten state to render a fully amorphous state with a glass transition temperature $T_g = 44\text{ }^\circ\text{C}$, as determined by calorimetry.

Polymer thin films were prepared by spin coating on silicon wafers (100) obtained from Wafer World Inc., which were polished on both surfaces. Before deposition, the substrates were cleaned in an ultrasonic bath with acetone and isopropanol. PTT was dissolved in trifluoroacetic acid (Sigma-Aldrich, reagent $\geq 98\%$) at a concentration of 15 g L^{-1} for 2 h at

room temperature. For thin film preparation, 0.2 mL of the polymer solution was dropped onto a square silicon substrate, typically measuring $2 \times 2\text{ cm}^2$. Immediately thereafter, the samples were spun for 2 min at 2400 rpm using a Laurell WS-650 series spin controller. These conditions yield spin-coated polymer films with a thickness of approximately 150 nm and an average surface roughness (R_a) of about 1 nm, as measured by AFM.

The light source for irradiation was a chirped pulsed amplified Ti: sapphire laser delivering 800 nm, 3 mJ, 50 fs linearly polarized pulses at a maximum repetition rate of 1 kHz. For this experiment, a maximum pulse energy of 600 μJ was employed, controlled by the combination of a half-wave plate and a polarizer. A 15 cm focal length spherical lens was installed in this near-infrared beam and the sample plane was situated 4 cm in front of the focal plane in such a way that the dimensions of the irradiation area were $2.4\text{ mm} \times 1.8\text{ mm}$ (1 e^{-2} diameter). Normal incidence was used in all cases. In this position, the maximum peak fluence on the sample was $\approx 35\text{ mJ cm}^{-2}$. The typical number of laser pulses applied to the same sample position was of the order of 10^4 . The repetition rate of the laser pulse train could be varied by adequately timing the output Pockels cell in the laser amplifier. For experiments requiring the use of temporally stretched pulses, the distance between the two diffraction gratings in the laser compressor was de-optimized, and thus pulses with positive or negative chirp could be obtained. The resulting time duration was monitored with a single-shot autocorrelator.

Surface topography was characterized by AFM in tapping mode. Measurements were done with an AFM Multimode 8 (Bruker®) with the controller Nanoscope V (Bruker®) and analysis was carried out using Nanoscope Analysis 1.9 software (Bruker®). For these measurements, silicon tips NSG30 (NT-MDT) with a curvature radius of $\approx 6\text{ nm}$, a nominal resonant frequency of 320 kHz, and a typical spring constant of 40 N m^{-1} , were used.

Acknowledgements

This work has been funded by the Spanish State Research Agency (AEI) through projects PID2019-106125GB-I00/AEI/10.13039/501100011033, PID2019-107514GB-I00/AEI/10.13039/501100011033, and PID2021-122839NB-I00. P.R. is grateful to Universidad Complutense de Madrid (UCM) for a Margarita Salas postdoctoral contract. I.M.C. is grateful to the Spanish Ministry of Universities for an FPU predoctoral contract (FPU21/04608). We thank Sandra Paszkiewicz and Anna Szymczyk for the preparation of the PTT. The facilities of the Center for Ultrafast Lasers (CLUR) of the Universidad Complutense de Madrid are gratefully acknowledged.

Conflict of Interest

The authors declare no conflict of interest.

Data Availability Statement

The data that support the findings of this study are available from the corresponding author upon reasonable request.

Keywords

chirp, femtosecond laser processing, laser-induced periodic surface structures (LIPSS), nanostructures, polymer thin films, repetition rate

Received: September 15, 2023

Revised: November 13, 2023

Published online:

- [1] M. Birnbaum, *J. Appl. Phys.* **1965**, *36*, 3688.
- [2] H. M. van Driel, J. E. Sipe, J. F. Young, *Phys. Rev. Lett.* **1982**, *49*, 1955.
- [3] J. Bonse, *Nanomaterials* **2020**, *10*, 1950.
- [4] J. Bonse, S. V. Kirner, J. Krüger, in *Handbook of Laser Micro-and Nano-Engineering*, Springer, Cham, Switzerland **2020**, p. 1, https://doi.org/10.1007/978-3-319-69537-2_17-1.
- [5] J. Bonse, S. Gräf, *Nanomaterials* **2021**, *11*, 3326.
- [6] F. Palumbo, C. Lo Porto, P. Favia, *Coatings* **2019**, *9*, 640.
- [7] A. F. Obilor, M. Pacella, A. Wilson, V. V. Silberschmidt, *Int. J. Adv. Manuf. Technol.* **2022**, *120*, 103.
- [8] R. I. Rodríguez-Beltrán, J. Prada-Rodrigo, A. Crespo, T. A. Ezquerra, P. Moreno, E. Rebollar, *Polymers* **2022**, *14*, 5243.
- [9] E. Rebollar, S. Pérez, J. J. Hernández, I. Martín-Fabiani, D. R. Rueda, T. A. Ezquerra, M. Castillejo, *Langmuir* **2011**, *27*, 5596.
- [10] I. Michaljaničová, P. Slepíčka, S. Rimpelová, N. Slepíčková Kasálková, V. Švorčík, *Appl. Surf. Sci.* **2016**, *370*, 131.
- [11] M. Mezera, M. van Drongelen, G. R. B. E. Römer, *J. Laser Micro/Nanoeng.* **2018**, *13*, 105.
- [12] M. Mezera, S. Alamri, W. A. P. M. Hendriks, A. Hertwig, A. M. Elert, J. Bonse, T. Kunze, A. F. Lasagni, G. R. B. E. Römer, *Nanomaterials* **2020**, *10*, 1184.
- [13] E. Rebollar, J. R. Vázquez de Aldana, J. A. Pérez-Hernández, T. A. Ezquerra, P. Moreno, M. Castillejo, *Appl. Phys. Lett.* **2012**, *100*, 041106.
- [14] E. Rebollar, J. R. Vázquez De Aldana, I. Martín-Fabiani, M. Hernández, D. R. Rueda, T. A. Ezquerra, C. Domingo, P. Moreno, M. Castillejo, *Phys. Chem. Chem. Phys.* **2013**, *15*, 11287.
- [15] Y. Jee, M. F. Becker, R. M. Walser, *J. Opt. Soc. Am. B* **1988**, *5*, 648.
- [16] E. Rebollar, M. Castillejo, T. A. Ezquerra, *Eur. Polym. J.* **2015**, *73*, 162.
- [17] C. Albu, A. Dinescu, M. Filipescu, M. Ulmeanu, M. Zamfirescu, *Appl. Surf. Sci.* **2013**, *278*, 347.
- [18] M. Mezera, J. Bonse, G. R. B. E. Römer, *Polymers* **2019**, *11*, 1947.
- [19] J. Cui, A. Nogaes, T. A. Ezquerra, E. Rebollar, *Appl. Surf. Sci.* **2017**, *394*, 125.
- [20] M. Csete, O. Marti, Z. Bor, *Appl. Phys. A* **2001**, *73*, 521.
- [21] P. Nürnberger, H. M. Reinhardt, H.-C. Kim, E. Pfeifer, M. Kroll, S. Müller, F. Yang, N. A. Hampp, *Appl. Surf. Sci.* **2017**, *425*, 682.
- [22] Y. Kalachyova, O. Lyutakov, P. Slepicka, R. Elashnikov, V. Svorcik, *Nanoscale Res. Lett.* **2014**, *9*, 591.
- [23] J. Prada-Rodrigo, R. I. Rodríguez-Beltrán, T. A. Ezquerra, P. Moreno, E. Rebollar, *Opt. Laser Technol.* **2023**, *159*, 109007.
- [24] A. San-Blas, M. Martínez-Calderon, E. Granados, M. Gómez-Aranzadi, A. Rodríguez, S. M. Olaizola, *Surf. Interfaces* **2021**, *25*, 101205.
- [25] J. Bonse, J. Krüger, *J. Appl. Phys.* **2010**, *108*, 34903.
- [26] P. Dzienny, B. Stępak, A. Budnicki, A. Antończa, *J. Laser Micro/Nanoeng.* **2020**, *15*, 12.
- [27] S. Bashir, M. S. Rafique, W. Husinsky, *Nucl. Instrum. Methods Phys. Res., Sect. B* **2015**, *349*, 230.
- [28] M. Kakehata, H. Yashiro, A. Oyane, A. Ito, K. Torizuka, in *Proc. SPIE* **2016**, p. 97401G, <https://doi.org/10.1117/12.2209013>.
- [29] M. Barberoglou, D. Gray, E. Magoulakis, C. Fotakis, P. A. Loukakos, E. Stratakis, *Opt. Express* **2013**, *21*, 18501.
- [30] T. J.-Y. Derrien, J. Krüger, T. E. Itina, S. Höhm, A. Rosenfeld, J. Bonse, *Appl. Phys. A* **2014**, *117*, 77.
- [31] F. Fraggelakis, G. Mincuzzi, J. Lopez, I. Manek-Hönninger, R. Kling, *Appl. Surf. Sci.* **2019**, *470*, 677.
- [32] J. Bonse, S. Hohm, V. S. Kirner, A. Rosenfeld, J. Kruger, S. V. Kirner, A. Rosenfeld, J. Kruger, *IEEE J. Sel. Top. Quantum Electron.* **2017**, *23*, 9000615.
- [33] S. Gräf, C. Kunz, S. Engel, T. J.-Y. Derrien, F. A. Müller, *Materials* **2018**, *11*, 1340.
- [34] L. Jiang, A.-D. Wang, B. Li, T.-H. Cui, Y.-F. Lu, *Light: Sci. Appl.* **2018**, *7*, 17134.
- [35] E. Allahyari, J. J. Nivas, M. Valadan, R. Fittipaldi, A. Vecchione, L. Parlato, R. Bruzzese, C. Altucci, S. Amoroso, *Appl. Surf. Sci.* **2019**, *488*, 128.
- [36] M. Hu, J. J. Nivas, M. Valadan, R. Fittipaldi, A. Vecchione, R. Bruzzese, C. Altucci, S. Amoroso, *Appl. Surf. Sci.* **2022**, *606*, 154869.
- [37] J. Prada-Rodrigo, *Ph.D. Thesis*, Salamanca University, **2023**.
- [38] S. Bashir, M. S. Rafique, C. S. Nathala, A. A. Ajami, W. Husinsky, K. Whitmore, *J. Opt. Soc. Am. B* **2020**, *37*, 2878.
- [39] J. Zhang, L. Zhang, W. Xu, *J. Phys. D: Appl. Phys.* **2012**, *45*, 113001.
- [40] P. Nürnberger, J. M. Reinhardt, H. Kim, E. Pfeifer, M. Kroll, S. Müller, F. Yang, N. A. Hampp, *Appl. Surf. Sci.* **2017**, *425*, 682.
- [41] A. Szymczyk, *Eur. Polym. J.* **2009**, *45*, 2653.